PHYSICAL REVIEW D **74,** 096005 (2006)

Nonperturbative part of the plaquette in pure gauge theory

Y. Meurice*

Department of Physics and Astronomy, The University of Iowa, Iowa City, Iowa 52242, USA

(Received 5 September 2006; published 16 November 2006)

We define the nonperturbative part of a quantity as the difference between its numerical value and the perturbative series truncated by dropping the order of minimal contribution and the higher orders. For the anharmonic oscillator, the double-well potential, and the single plaquette gauge theory, the nonperturbative part can be parametrized as $A\lambda^B e^{-C/\lambda}$ and the coefficients can be calculated analytically. For lattice QCD in the quenched approximation, the perturbative series for the average plaquette is dominated at low order by a singularity in the complex coupling plane and the asymptotic behavior can only be reached by using extrapolations of the existing series. We discuss two extrapolations that provide a consistent description of the series up to order 20–25. These extrapolations favor the idea that the nonperturbative part scales like $(a/r_0)^4$ with a/r_0 defined with the force method. We discuss the large uncertainties associated with this statement. We propose a parametrization of $\ln(a/r_0)$ as the two-loop universal terms plus a constant and exponential corrections. These corrections are consistent with $a^2_{\text{1-loop}}$ and play an important role when $\beta < 6$. We briefly discuss the possibility of calculating them semiclassically at large β.

DOI: 10.1103/PhysRevD.74.096005 PACS numbers: 11.15.−q, 11.15.Ha, 11.15.Me, 12.38.Cy

I. INTRODUCTION

The perturbative renormalizability of the standard model is a remarkable property that played an important role in establishing its phenomenological prominence. It guarantees that we can calculate the radiative corrections at any order in perturbation theory. However, Dyson's argument [1] suggests that these perturbative series are divergent and one needs to truncate them in order to get a finite result. A procedure often used for this purpose consists in dropping the smallest contribution at a given coupling and all the higher order terms. The difference between this truncated series and the numerical value of the quantity calculated can be called the nonperturbative part (NPP). The NPP depends on the truncation procedure and also on the renormalization scheme. However, if the NPP has a simple parametrization and if we can calculate it approximately, we will have made a big step toward a complete solution of the problem.

In this article, we discuss the NPP as defined above for a variety of models. Our main goal is to find an accurate formula for the average plaquette in lattice QCD in the quenched approximation. The paper is organized as follows. In Sec. II, we calculate the minimal error that can be made at a given coupling, if we assume that for sufficiently small coupling the error is dominated by the first order dropped. In Sec. III, we show that the general estimates of Sec. II work well for the anharmonic oscillator. In Sec. IV, we show that, for the ground state of the double-well potential, the one instanton effect is larger than the error estimated on the basis of the asymptotic behavior of the perturbative series. However, for the average of the two lowest energy levels, we obtain a good agreement with the general estimate. The case of a $SU(2)$ lattice gauge theory with one plaquette is discussed in Sec. V. In that case, the NPP can be calculated exactly and it can be checked that the error formula works well. In contrast to what happens for the anharmonic oscillator where the error at a given order has a given sign, the examples discussed in Secs. IV and V show more complicated sign patterns that can be studied easily because we can calculate the numerical values very accurately. In particular, Figs. 1–9 should be understood as a tutorial for the interpretation of Figs. 14 and 15.

In all the above examples, the NPP can be approximated as $A\lambda^B e^{-C/\lambda}$ with λ a generic notation for the expansion parameter. Could the same type of result be obtained in lattice gauge theory? Lattice QCD in the quenched approximation is introduced in Sec. VI. Simple hypotheses (power of the two-loop renormalization invariant scale, power of the lattice spacing) for the NPP of the plaquette are compared with the numerical data using a series calculated up to order 10 [2]. This order is not large enough to decide if any of the hypotheses are adequate. Higher order extrapolations are necessary to discriminate among the various possibilities. In Sec. VII, two extrapolations are discussed. One is based on the existence of complex singularities [3], the other on the existence of an infrared renormalon [4–6]. These two extrapolations predict quite correctly the 16th coefficient as it can be obtained from a graph in Ref. [7]. They both seem consistent with the possibility [7,8] that the NPP is proportional to the 4th power of the lattice spacing as parametrized using the force method in Refs. [9,10]. The uncertainties associated with the extrapolations are discussed in Sec. VIII. In Sec. IX, we discuss an exponential parametrization of the lattice spacing as a function of the inverse coupling. Our result is consistent with the possibility of corrections scaling ap-

*Electronic address: yannick-meurice@uiowa.edu

proximately like $a^2_{\text{1-loop}}$, in good agreement with a suggestion made in Ref. [11]. In the Conclusions, we discuss the possibility of calculating the corrections semiclassically.

Some words of caution, the separation between the NPP and the truncated series is a computational scheme. We do not claim that the NPP has a distinct physical interpretation. In the past, there have been attempts [6–8,12] to relate the difference between the average plaquette and its perturbative expansion to the gluon condensate used in calculations based on the operator product expansion (OPE) in the continuum. The results presented here can certainly be compared to the lattice calculations in these references; however, our goal is to understand a particular lattice model studied with a particular perturbative scheme. We believe that an accurate parametrization of the NPP, defined above as a function of β, is a preliminary step that needs to be completed before attempting to extract accurate numerical values of continuum quantities such as the gluon condensate.

II. MINIMAL ERROR ESTIMATE

In the following, we consider quantities Q which admit an asymptotic series of the form

$$Q \sim \sum_{k=0}^{\infty} a_k \lambda^k. \tag{1}$$

We assume that the leading growth of the coefficients can be parametrized as follows:

$$a_k \sim C_1 C_2^k \Gamma(k + C_3). \tag{2}$$

This type of behavior is justified generically in Ref. [13]. In the case of lattice gauge theory, this type of behavior is seen explicitly in the limiting case of the one plaquette model discussed in Sec. V. We define Δ_k as the difference between the numerical value of Q and the series truncated at order k:

$$\Delta_k(\lambda) \equiv Q(\lambda) - \sum_{l=0}^{k} a_l \lambda^l. \tag{3}$$

In addition, we will assume that, for sufficiently small coupling, Δ_k is approximately given by the next order contribution

$$\Delta_k \simeq \lambda^{k+1} a_{k+1}. \tag{4}$$

At fixed coupling λ, $|\Delta_k|$ can then be minimized for $k = k^\star$ with

$$k^\star \simeq (\lambda|C_2|)^{-1} - C_3 - (1/2) + \mathcal{O}(\lambda|C_2|). \tag{5}$$

This expression has been obtained by using the leading term of the Stirling formula for the gamma function $(\sqrt{2\pi} z^{z-1/2} \mathrm{e}^{-z})$. In Eq. (5), $(\lambda|C_2|)^{-1}$ is the leading term and $-C_3 - (1/2)$ the first correction. It assumed that λ is small enough to neglect the $\mathcal{O}(\lambda|C_2|)$ terms which require the higher order terms of the Stirling formula. Plugging Eq. (5) in the expected error gives the minimal error,

$$\min_k |\Delta_k| \simeq \sqrt{2\pi}|C_1|(\lambda|C_2|)^{1/2-C_3} \mathrm{e}^{-(1/|C_2|\lambda)}. \tag{6}$$

The exponential part of this formula is well known [13].

III. THE ANHARMONIC OSCILLATOR

A simple quantum mechanics example where the situation described in Sec. II is approximately realized is the anharmonic oscillator. The Hamiltonian reads

$$H = p^2/2 + x^2/2 + \lambda x^4. \tag{7}$$

We discuss the perturbative expansion of the ground state energy

$$E_0 \sim \sum_{k=0} a_k \lambda^k. \tag{8}$$

The leading asymptotic behavior of the coefficients has been calculated by Bender and Wu [14]:

$$a_k \sim (-1)^{k+1} \sqrt{6/\pi^3}\, 3^k \Gamma(k + 1/2). \tag{9}$$

Using Eq. (6), we obtain

$$\min_k |\Delta_k| \simeq (\sqrt{12}/\pi) \mathrm{e}^{-(1/3\lambda)}. \tag{10}$$

This is illustrated in Fig. 1 where the logarithm of the error

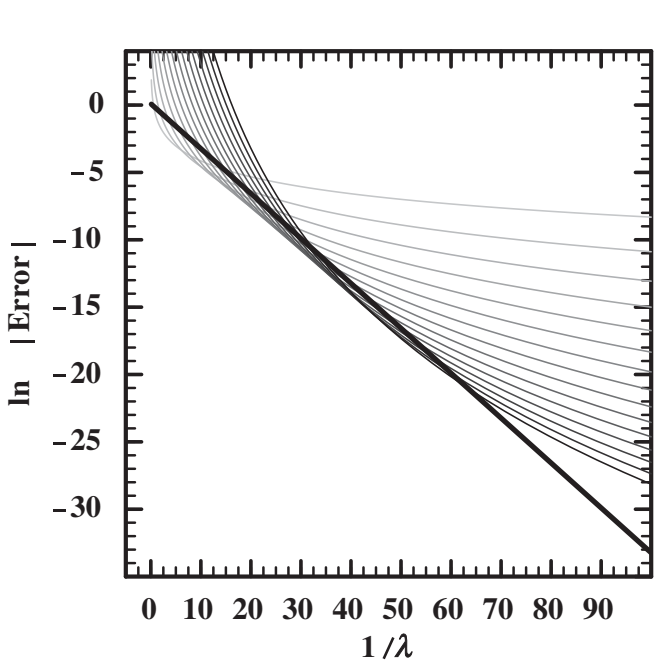

FIG. 1. Natural logarithm of the absolute value of the difference between the series and the numerical value for order 1 to 15 for the anharmonic oscillator as a function of $1/\lambda$. As the order increases, the curves get darker. The thicker dark curve is $\ln((\sqrt{12}/\pi)\mathrm{e}^{-(1/3\lambda)})$.

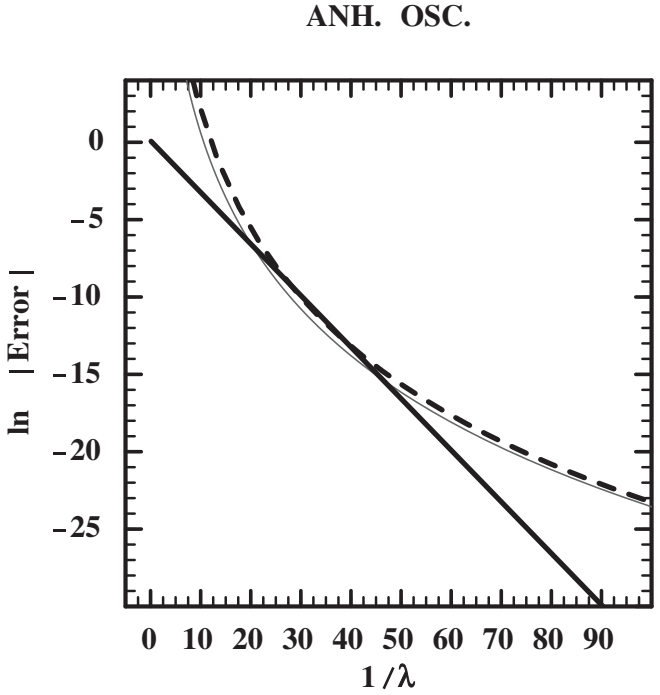

FIG. 2. Natural logarithm of the absolute value of the difference between the series and the numerical value for order 10 as in Fig. 1 compared with the estimate of Eq. (4) at order 10 (dashes). The thicker dark curve is $\ln((\sqrt{12}/\pi)e^{-(1/3\lambda)})$.

is plotted versus $1/\lambda$. With this choice of variables, the minimal error is represented by a straight line that is approximately tangent to all the curves representing the empirical error.

A careful look at Fig. 1 shows that the empirical curves go slightly below our estimated error. In other words, $|\Delta_k|$ is slightly smaller than Eq. (4). This is illustrated in Fig. 2. One can see that the minimal error from Eq. (10) provides an envelope for the curves from Eq. (4) at various order, but the empirical $|\Delta_k|$ are slightly smaller. One also sees that Eq. (4) becomes better as λ becomes smaller. A more detailed study shows that the difference between Eq. (4) and $|\Delta_k|$ decreases as a power of λ close to 1. The features of $|\Delta_k|$ seem related to the fact that the series has alternated signs. In the following, we will only consider same sign series. Understanding the above feature is not crucial for the rest of the discussion.

IV. THE DOUBLE WELL

A more intricate situation in encountered for the double-well potential. In shifted coordinates, the potential reads

$$V(y) = (1/2)y^2 - gy^3 + (g^2/2)y^4. \tag{11}$$

If we expand the ground state in powers of g^2,

$$E_0 \sim \sum_{k=0} a_k g^{2k}, \tag{12}$$

the leading asymptotic behavior of the coefficients reads [15]

$$a_k \sim -(3/\pi)3^k\Gamma(k+1). \tag{13}$$

This implies

$$\min_k |\Delta_k| \simeq \sqrt{6/\pi}\, g^{-1} e^{-(1/3g^2)}. \tag{14}$$

Figure 3 shows that this lower bound on the error is not reached. Rather, we see that the error is bounded by the one instanton contribution

$$\Delta E_0 = -(g\pi)^{-1/2} e^{-(1/6g^2)}. \tag{15}$$

This is a nonperturbative effect that at first sight is not related to the large order behavior of the perturbative series. However, some connection exists (see below).

As illustrated in Fig. 4, a good approximation for the error at order k is

$$\Delta_k \simeq -(g\pi)^{-1/2} e^{-(1/6g^2)} + a_{k+1} g^{2(k+1)}. \tag{16}$$

Both terms are negative and there is no possible cancellation between them.

Except for the overall normalization, Eq. (14) is the square of the instanton effect. This is not a coincidence. In Ref. [15], it is explained that Eq. (13) is an instanton–anti-instanton effect. It is possible to get rid of the one

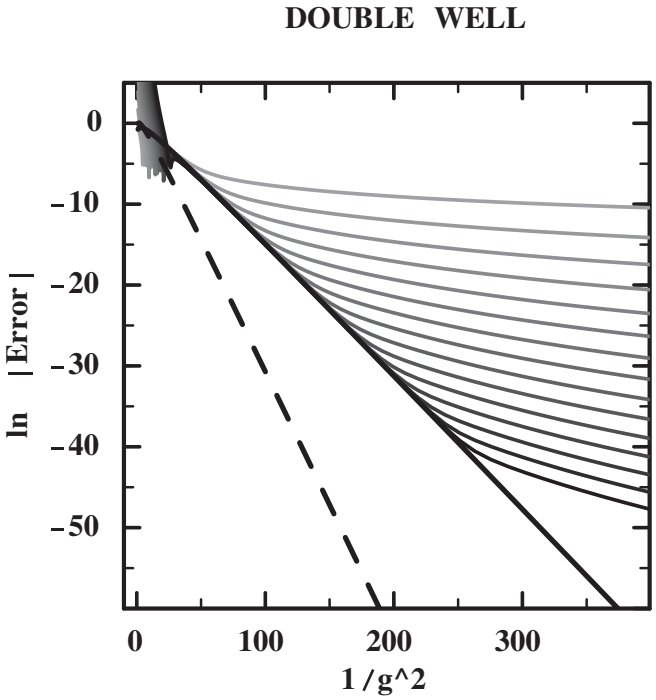

FIG. 3. Natural logarithm of the absolute value of the difference between the series and the numerical value for order 1 to 15 (in g^2) versus $1/g^2$ for the ground state of the double-well potential. As the order increases, the curves get darker. The thicker dark curve is $\ln((g\pi)^{-1/2}e^{-(1/6g^2)})$. The dashed curve is $\ln(\sqrt{6/\pi}g^{-1}e^{-(1/3g^2)})$.

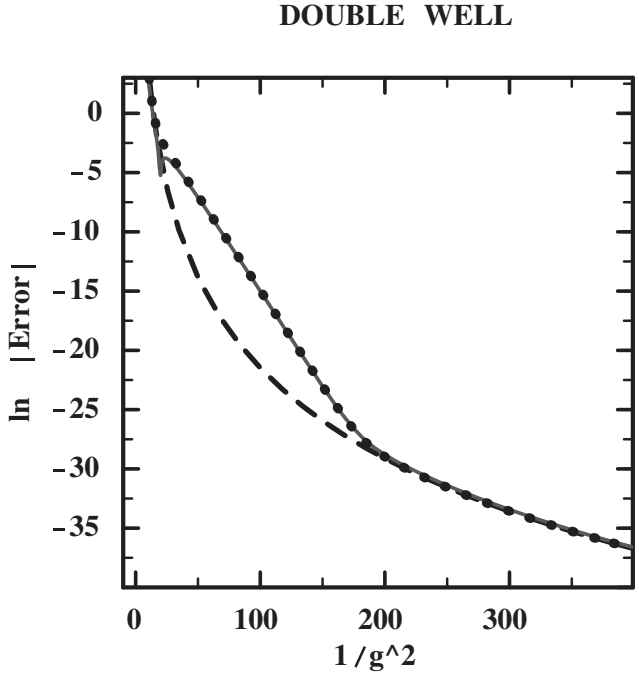

FIG. 4. Natural logarithm of the absolute value of the difference between the series and the numerical value for order 10 (in g^2) versus $1/g^2$ for the ground state of the double-well potential (solid line). The long dashed curve is $\ln(|a_{11}g^{22}|)$. The dots represent $\ln(|-(g\pi)^{-1/2}e^{-(1/6g^2)}+a_{11}g^{22}|)$.

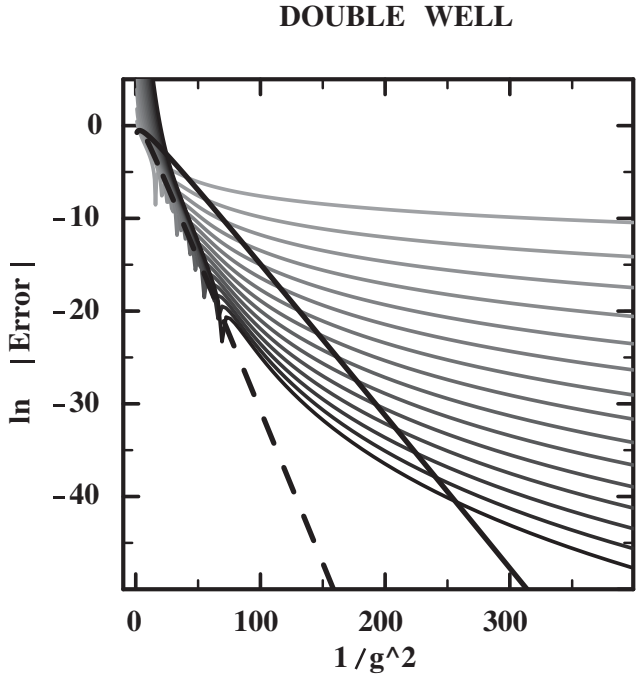

FIG. 5. Natural logarithm of the absolute value of the difference between the series and the numerical value for order 1 to 10 (in g^2) versus $1/g^2$ for the average between the two lowest energy states of the double-well potential. As the order increases, the curves get darker. The thicker dark curve is $(g\pi)^{-1/2}e^{-(1/6g^2)}$. The dashed curve is $\sqrt{6/\pi}g^{-1}e^{-(1/3g^2)}$.

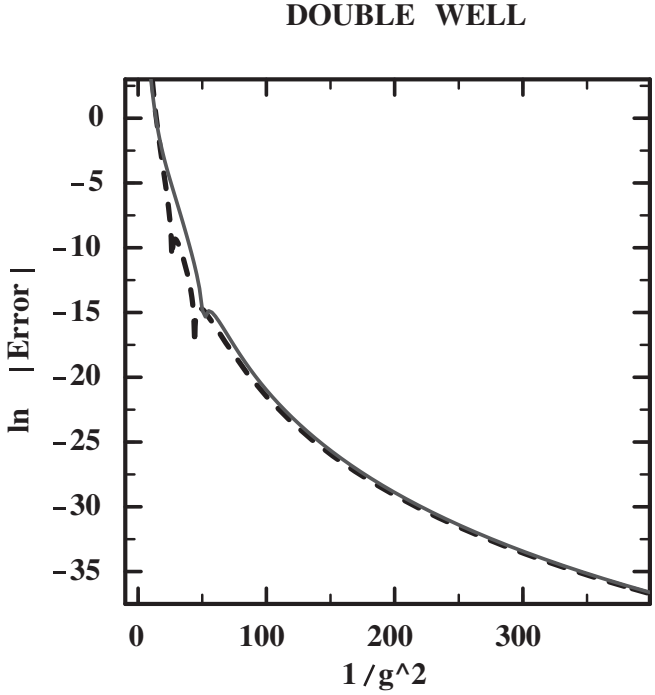

FIG. 6. Natural logarithm of the absolute value of the difference between the series and the numerical value for order 10 (in g^2) versus $1/g^2$ for the average of the two lowest states of the double-well potential (solid line). The dashed curve is $\ln(|\sqrt{6/\pi}g^{-1}e^{-(1/3g^2)}+a_{11}g^{22}|)$.

instanton effect by replacing the numerical value of the ground state by an average over the two lowest energy levels. This can be seen from the lowest order semiclassical formula [16]:

$$E_0 \simeq (1/2) - (g\pi)^{-1/2}e^{-(1/6g^2)},$$
$$E_1 \simeq (1/2) + (g\pi)^{-1/2}e^{-(1/6g^2)}.$$

One then recovers Eq. (14) as shown in Fig. 5. Note that the approximate doubling of the energy levels at small coupling is not seen in perturbation theory because one minimum of the potential goes to infinity when g goes to zero.

As illustrated in Fig. 6, a good approximation for the error at order k on the average of the two lowest energy states is

$$\Delta_k^{\mathrm{av}} \simeq \sqrt{6/\pi}g^{-1}e^{-(1/3g^2)} + a_{k+1}g^{2(k+1)}. \qquad (17)$$

The two terms are of opposite signs and there are possible cancellations between them. This explains the spikes seen in Figs. 5 and 6.

V. A ONE PLAQUETTE GAUGE MODEL

Before discussing quenched QCD, we consider the single plaquette $SU(2)$ gauge theory. After gauge fixing three of the four links, the partition function reads

$$Z(\beta) = \int dU e^{-\beta(1-(1/2)\,\mathrm{Re\,Tr}\,U)}. \quad (18)$$

Assuming $\beta > 0$, this can be rewritten as

$$Z(\beta) = (2/\beta)^{3/2}\frac{1}{\pi}\int_0^{2\beta} dt t^{1/2} e^{-t}\sqrt{1-(t/2\beta)}. \quad (19)$$

In Ref. [17], it is shown that the integral can be expressed exactly as a converging expansion in β^{-1}:

$$Z(\beta) = (\beta\pi)^{-3/2}2^{1/2}\sum_{k=0}^{\infty} A_k(2\beta)\beta^{-k}, \quad (20)$$

with

$$A_k(x) \equiv 2^{-k}\frac{\Gamma(k+1/2)}{k!(1/2-k)}\int_0^x dt e^{-t}t^{k+1/2}. \quad (21)$$

Note that the peak of the integrand $e^{-t}t^{k+1/2}$ becomes larger than 2β when $k = 2\beta - 1/2$; consequently, the expansion is approximately truncated at that order. On the other hand, if we extend the range of integration from 2β to $+\infty$, the integral in Eq. (21) becomes the gamma function and the coefficients grow factorially. We can determine the parameters C_1, C_2, and C_3 of the leading asymptotic behavior given in Eq. (2). We consider the sum *without* the prefactor $(\beta\pi)^{-3/2}2^{1/2}$. From the study of ratios of successive coefficients, we obtain $C_2 = 1/2$ and $C_3 = 0$. Using Stirling formula, we then obtain $C_1 = 1$. From Eq. (5), the optimal order of truncation is

$$k^\star = 2\beta - 1/2. \quad (22)$$

Note that this is exactly the same order as the order where the peak of the integrand moves outside of the range of integration in the exact Eq. (21). From Eq. (6) and after restoring the prefactor, we obtain

$$\min_k|\Delta_k| \simeq (2^{1/2}/\pi)\beta^{-2}e^{-2\beta}. \quad (23)$$

Figure 7 shows that this is a good approximation.

It is now possible to define precisely what we mean by "the nonperturbative part of $Z(\beta)$." The perturbative part is the perturbative series [Eq. (21) with the argument of A_k replaced by ∞] truncated at the integer closest to $k^\star$ defined above, and denoted $r(k^\star)$ hereafter. The nonperturbative part consists of two parts. The first part, denoted R, consists in the remaining terms of orders $r(k^\star)+1$ and higher in Eq. (20). The second part, denoted T, is minus the integration tails for the first $r(k^\star)$ terms that we have added in order to get a perturbative series in $1/\beta$ with β-independent coefficients. More explicitly,

$$Z(\beta) = Z_{\mathrm{pert}}(\beta) + Z_{N\,\mathrm{pert}}(\beta), \quad (24)$$

with

$$Z_{\mathrm{pert}}(\beta) = (\beta\pi)^{-3/2}2^{1/2}\sum_{k=0}^{r(k^\star)} A_k(\infty)\beta^{-k}, \quad (25)$$

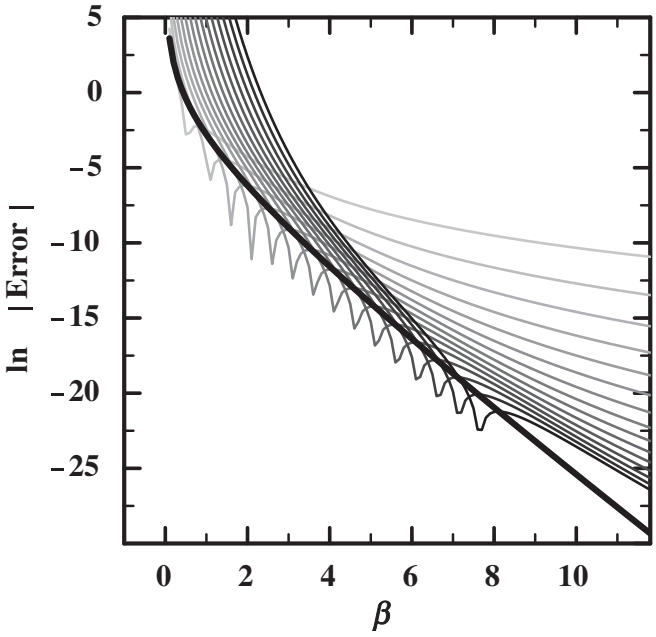

FIG. 7. Natural logarithm of the absolute value of the difference between the series and the numerical value for order 1 to 10 for the one plaquette integral as a function of β. As the order increases, the curves get darker. The thicker dark curve is $\ln((2^{1/2}/\pi)e^{-2\beta}/\beta^2)$.

and

$$Z_{N\,\mathrm{pert}}(\beta) = (R(\beta) - T(\beta)) \quad (26)$$

$$R(\beta) = (\beta\pi)^{-3/2}2^{1/2}\sum_{r(k^\star)+1}^{\infty} A_k(2\beta)\beta^{-k} \quad (27)$$

$$T(\beta) = (\beta\pi)^{-3/2}2^{1/2}\sum_{k=0}^{r(k^\star)}\beta^{-k}\frac{\Gamma(k+1/2)}{k!(1/2-k)} \times \int_{2\beta}^{\infty} dt e^{-t}t^{k+1/2}. \quad (28)$$

The asymptotic behavior of $T(\beta)$ can be estimated using Sec. VI of Ref. [17]. We obtained that, at leading order, the contribution of the tails up to order K is

$$\delta Z(\beta, K) \approx A_K e^{-2\beta}\beta^{-1}2\pi^{-3/2}, \quad (29)$$

with

$$A_K = -\sum_{l=0}^{K}\frac{\Gamma(l-1/2)}{l!}. \quad (30)$$

Writing $(1-e^{-t})$ as $e^{-t}(e^t-1)$ and expanding e^t, we obtain

$$\sum_{l=1}^{\infty} \frac{\Gamma(l-1/2)}{l!} = \int_0^{\infty} dt t^{-3/2}(1-e^{-t}) = 2\pi^{1/2}. \quad (31)$$

For large K,

$$\sum_{l=1}^{K} \frac{\Gamma(l-1/2)}{l!} \simeq \int_0^{K} dt t^{-3/2}(1-e^{-t}), \quad (32)$$

we obtain the leading behavior

$$A_K \simeq \int_K^{\infty} dt t^{-3/2} = 2K^{-1/2}. \quad (33)$$

Replacing K by its optimal value in Eq. (22), we conclude that for large β

$$T(\beta) \simeq (2/\pi)^{3/2}\beta^{-3/2}e^{-2\beta}. \quad (34)$$

It is interesting to notice that $T(\beta)$ is larger by a factor $\beta^{1/2}$ than the estimated error given in Eq. (6). This means that we should also have

$$R(\beta) \simeq (2/\pi)^{3/2}\beta^{-3/2}e^{-2\beta} \quad (35)$$

so that the two leading order contributions cancel. The correctness of this argument is illustrated in Figs. 8 and 9.

In conclusion, we have learned that, in this simple lattice model with a compact gauge group, the nonperturbative part of the integral has two pieces. One piece comes from the higher orders, is positive, and dominates at sufficiently large β. The other comes from the added tails of integration, is negative, and dominates at sufficiently small β. It is possible that this pattern persists for the usual lattice gauge models on cubic lattices.

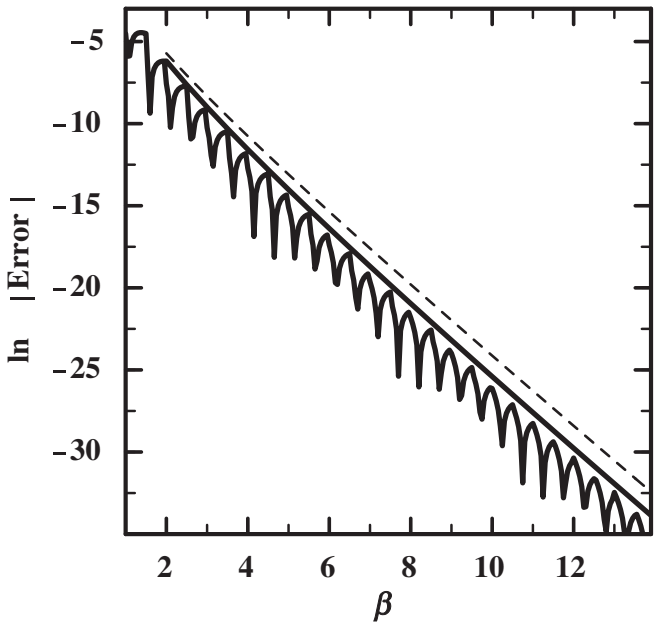

FIG. 8. $\ln|R(\beta) - T(\beta)|$ versus β (lowest, wavy line). The intermediate, almost straight curve is $\ln((2^{1/2}/\pi)\beta^{-2}e^{-2\beta})$. The dashed curve is $\ln((2/\pi)^{3/2}\beta^{-3/2}e^{-2\beta})$.

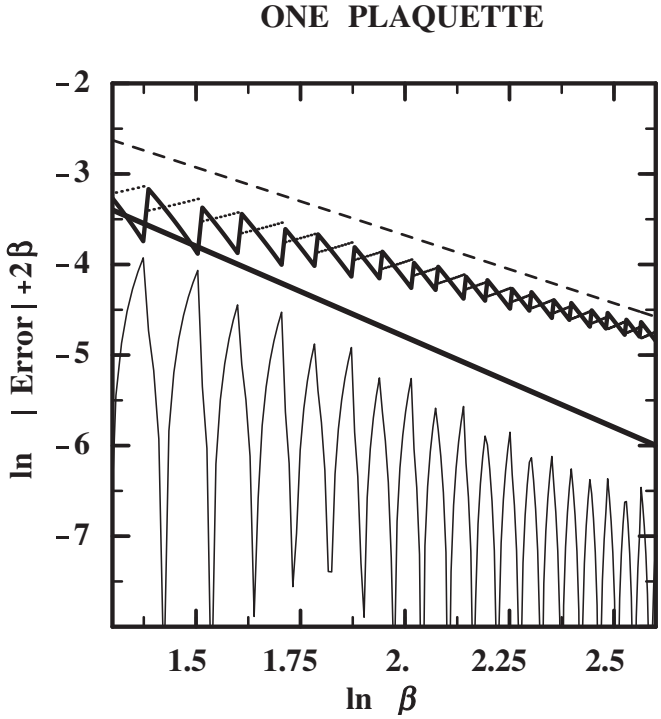

FIG. 9. $\ln|R(\beta) - T(\beta)| + 2\beta$ versus $\ln(\beta)$ (wavy curve in the lower part of the graph). The thicker line is $\ln((2^{1/2}/\pi)/\beta^2)$. The dashed line is $\ln((2/\pi)^{3/2}\beta^{-3/2})$. $\ln|R(\beta)| + 2\beta$ (points) and $\ln|T(\beta)| + 2\beta$ (line) are interweaved between the two straight lines.

VI. QUENCHED QCD

We now proceed to introduce lattice quenched QCD, the main model discussed in this article. With standard notations, the partition function is

$$Z = \prod_l \int dU_l e^{-\beta\sum_p (1-(1/N)\,\mathrm{Re\,Tr}\,(U_p))} \quad (36)$$

with $\beta = 2N/g^2$. For symmetric finite lattices with L^D sites and periodic boundary conditions, the number of plaquettes is

$$\mathcal{N}_p \equiv L^D D(D-1)/2. \quad (37)$$

Using the free energy density

$$f \equiv -(1/\mathcal{N}_p)\ln Z, \quad (38)$$

we define the average plaquette

$$P = \partial f/\partial\beta, \quad (39)$$

and its perturbative expansion

$$P(\beta) \sim \sum_{m=1} b_m \beta^{-m}. \quad (40)$$

In the following, we used the first three analytical values from Ref. [18], and the coefficients from 4 to 10 from Ref. [2]. The coefficients of Ref. [7] up to order 16 are given in a figure and will be used to check extrapolations. At large β, high precision data is necessary and we have used some values of the average plaquette from Refs. [19,20].

A simple guess is that the envelope of the accuracy curves is given by a power of some renormalization group invariant scale. For instance, one could test the idea that it is proportional to the fourth power of the two-loop renormalization group invariant scale

$$\min_k |\Delta_k| \simeq C(\beta)^{204/121} e^{-(16\pi^2/33)\beta}. \quad (41)$$

Figure 10 shows that, up to order 10, this provides a reasonable envelope in the region $5.5 < \beta < 6$. The constant C has been fixed to 6.5×10^8 by finding a plateau in $|\Delta_{10}|(\beta)^{-204/121} e^{(16\pi^2/33)\beta}$. As the curves leave the conjectured envelope, they become more flat. For instance at order 8 and for $6 < \beta < 7$, a reasonable fit can be obtained [6] with the square of the perturbative renormalization invariant scale. However, this does not seem to characterize the asymptotic behavior.

Note also that, at values of β close to 6, the empirical error is significantly larger than the next order contribution. This is illustrated in Fig. 11 at order 5.

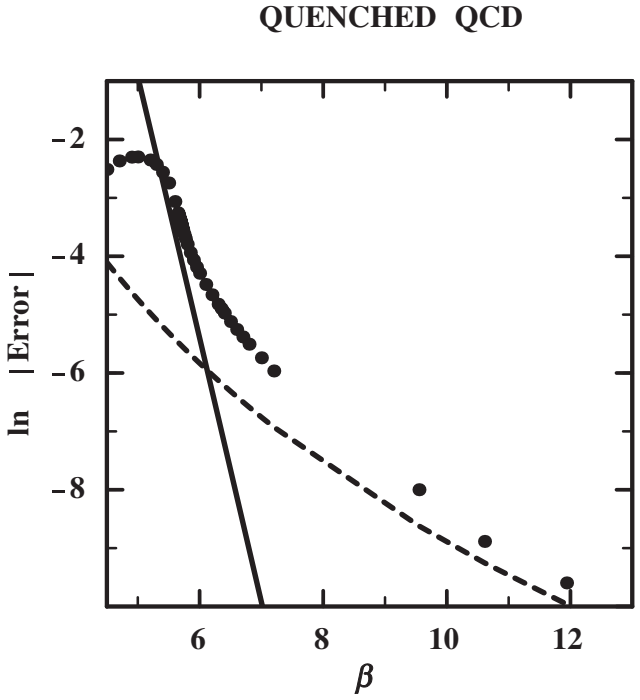

FIG. 11. Natural logarithm of the absolute value of the difference between the series and the numerical value for order 5 for quenched QCD as a function of β (dots). The dash line is $\ln(|a_6/\beta^6|)$. The solid curve is $\ln(6.5 \times 10^8 \times (\beta)^{204/121} e^{-(16\pi^2/33)\beta})$.

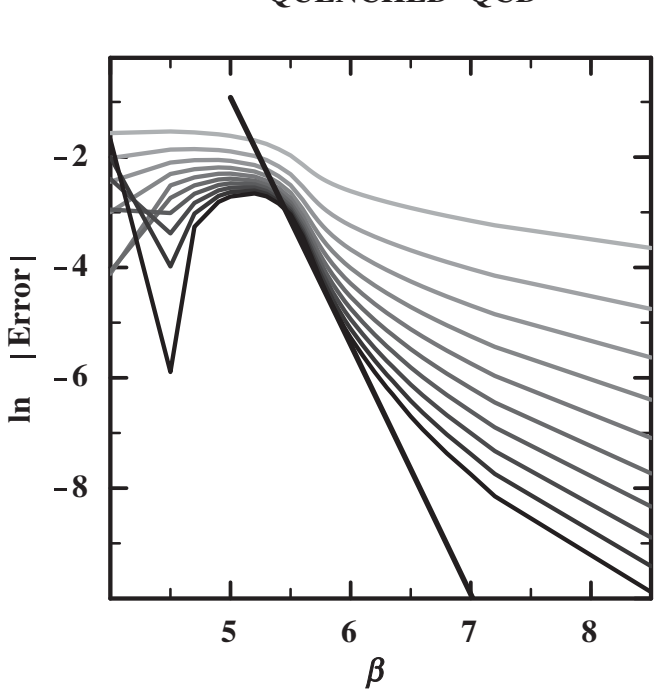

FIG. 10. Natural logarithm of the absolute value of the difference between the series and the numerical value for order 1 to 10 for quenched QCD as a function of β. As the order increases, the curves get darker. The approximately straight dark curve is $\ln(6.5 \times 10^8 \times (\beta)^{204/121} e^{-(16\pi^2/33)\beta})$.

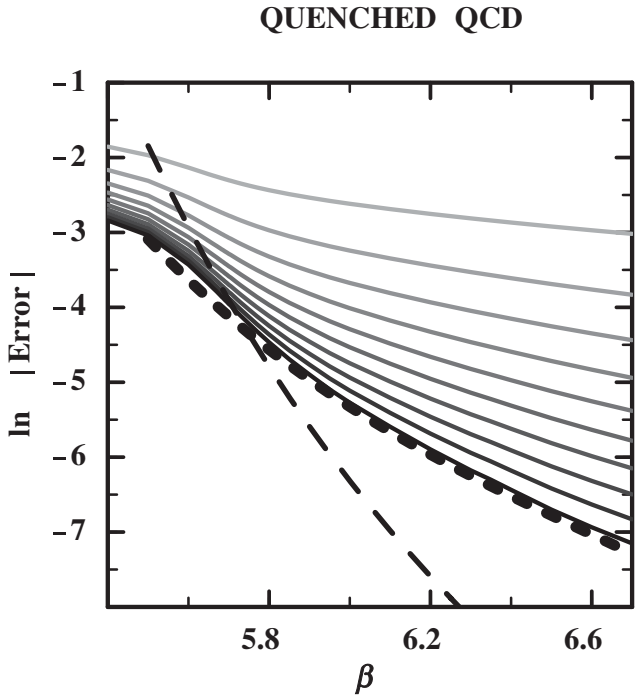

FIG. 12. Natural logarithm of the absolute value of the difference between the series and the numerical value for order 1 to 10 for quenched QCD as a function of β. As the order increases, the curves get darker. The short dashed curve is $\ln(0.14(a/r_0)^2)$. The long dashed curve is $\ln(1.5(a/r_0)^4)$.

Another simple guess is that the envelope is proportional to a power of the lattice spacing a expressed in units of $r_0 = 0.5$ fm. For the interval $5.7 < \beta < 6.92$, the following empirical power series [10] was obtained from the force method:

$$\ln(a/r_0) = -1.6804 - 1.7331(\beta - 6) + 0.7849(\beta - 6)^2 - 0.4428(\beta - 6)^3.$$

It has been suggested that the envelope is proportional to a^4 [7,8,12], however this is hard to establish without the knowledge of the higher orders. On the other hand, the accuracy curve at order 10 can be fitted very well with a^2 but again it does not seem to characterize the asymptotic behavior since the successive orders are still quite separated. This is illustrated in Fig. 12.

The question is now, if the higher orders can be calculated will the envelope stay approximately straight as in Fig. 10 or curl up as in Fig. 12? These two alternatives need to be compared systematically. As we will see in the next section, this requires the knowledge of coefficients of higher orders than those actually calculated.

VII. LARGE ORDER EXTRAPOLATIONS

In this section, we consider two large order extrapolations that can be built out of the first 10 terms used above. The first extrapolation is based on the assumption justified in Ref. [3] that $\partial P/\partial\beta$ has a logarithmic singularity in the complex β plane. Integrating, we obtain

$$\sum_{k=1} a_k \beta^{-k} \simeq C(\mathrm{Li}_2(\beta^{-1}/(\beta_m^{-1} + i\Gamma)) + \mathrm{H.c}, \qquad (42)$$

with

$$\mathrm{Li}_2(x) = \sum_{k=1} x^k/k^2. \qquad (43)$$

In Ref. [3] we argued that $0.001 < \Gamma < 0.01$ and, for this range of values, the low order coefficients depend very little on Γ. For this reason, it is difficult to fit its value given the accuracy of the coefficients. We have taken the intermediate value $\Gamma = 0.003$ which is compatible with everything we know and determined $C = 0.0654$ and $\beta_m = 5.787$ using the known values of a_9 and a_{10} on a 24^4 lattice [2]. The estimated errors on these coefficients and their impact on the determination of C and β_m are discussed at length in the next section. Other choices of Γ with this order of magnitude do not affect our conclusions. The numerical values are given in Table I. Except for the first term, the agreement is very good. The fact that such a good agreement can be reached by tuning two parameters begs for a diagrammatic explanation.

We also obtained $a_{16} = 7.7 \times 10^8$. This is quite close to what we found from Fig. 1 in Ref. [7]: $a_{16} \simeq 0.000\,27 \times 6^{16} \simeq 7.6 \times 10^8$. Note however, that this value of a_{16} was obtained on a 8^4 lattice and the finite volume effects should be significant. The perturbative series obtained from Eq. (42) has finite radius of convergence [3,8]. This seems to contradict the common wisdom [21] that if we ignore nonperturbative effects (responsible for the fact that P takes different limits [22] when $g^2 \to 0^{\pm}$), we should run into much more serious problems. Consequently, we believe that Eq. (42) can only be a good model for the low orders.

TABLE I. b_m: regular coefficients; $\tilde{b}_m$: extrapolated coefficients for $\Gamma = 0.003$.

m	b_m	$\tilde{b}_m$
1	2	0.7567
2	1.2208	1.094
3	2.9621	2.811
4	9.417	9.138
5	34.39	33.79
6	136.8	135.5
7	577.4	575.1
8	2545	2541
9	11 590	11 590
10	54 160	54 160

Models based on infrared renormalons [4–6] have a better chance to reproduce the large order behavior of the series. We assume

$$P \approx K \int_{t_1}^{t_2} dt e^{-\bar{\beta}t}(1 - t33/16\pi^2)^{-1-x} \qquad (44)$$

with

$$\bar{\beta} = \beta(1 + d_1/\beta + \cdots). \qquad (45)$$

In Refs. [4,6], the value $x = 204/121$ was used. Note that $t_1 = 0$ corresponds to the UV cutoff (we use that value later) and $t_2 = 16\pi^2/33$ corresponds to the Landau pole. Expanding $(1 - t33/16\pi^2)^{-1-x}$ in powers of t and extending the integration range to ∞, we find that at leading order

$$P(\beta) \sim \sum_{m=1} \bar{b}_m \bar{\beta}^{-m}, \qquad (46)$$

with

$$\bar{b}_k = C_1(33/16\pi^2)^k \Gamma[k + x]. \qquad (47)$$

Setting d_2 and higher order coefficients to zero, $x = 204/121$, and using the known values of a_9 and a_{10}, we obtain $C_1 = 0.219$ and $d_1 = -3.82$. The low order predictions are less good than for the previous method, for instance, $a_6 = 120.4$. At larger order we obtained $a_{16} = 7.4 \times 10^8$ which is close to 7.6×10^8. Note that $e^{4\pi^2(3.82)/33} \simeq 97$ is significantly larger than the usual [23] factor 28.81 found for the conversion to the $\overline{\mathrm{MS}}$ scheme.

The two extrapolation models are compared in Fig. 13. The two models yield similar coefficients up to order 20.

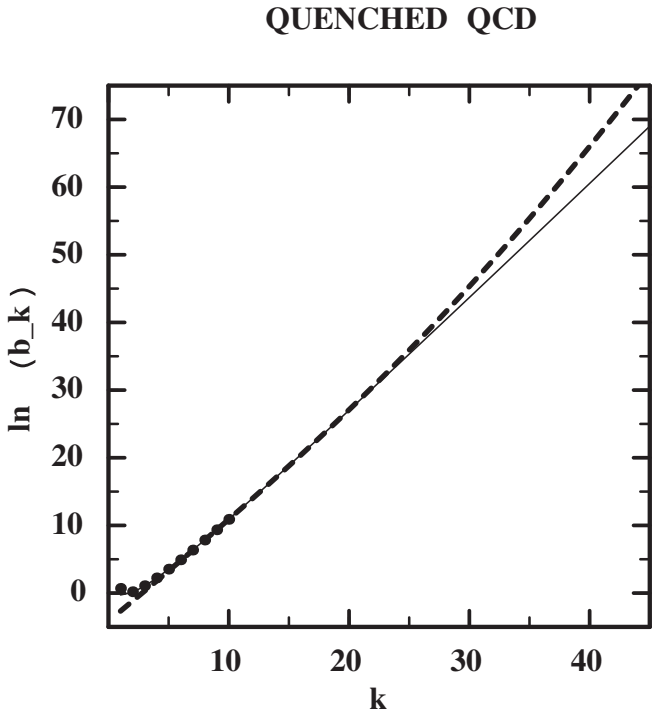

FIG. 13. $\ln(b_k)$ for the dilogarithm model (solid line) and the integral model (dashes). The dots up to order 10 are the known values.

After that, the integral model has the logarithm of its coefficients growing faster than linear.

Using Eq. (6), for the $\bar{\beta}^{-1}$ expansion, we obtain

$$\min_k|\Delta_k| \simeq 3.5(\bar{\beta})^{204/121-1/2}e^{-(16\pi^2/33)\bar{\beta}}. \quad (48)$$

Shifting to β using Eq. (45) and neglecting β^{-1} corrections,

$$\min_k|\Delta_k| \simeq 3.110^8(\beta)^{204/121-1/2}e^{-(16\pi^2/33)\beta}. \quad (49)$$

Except for the $-1/2$ in the exponent, this is proportional to the two-loop renormalization group invariant. The situation is reminiscent of what we encountered in Sec. V where the error was smaller by a factor $\beta^{-1/2}$ than naively expected. Another possibility would be to take $x = 204/121 + 1/2$ if we insist on having a quantity that is scheme independent.

The study of the asymptotic behavior of the empirical β^{-1} expansion between orders 40 and 60 indicates $C_2 \simeq 0.203$ quite close to $33/(16\pi^2) \simeq 0.209$. The other values obtained are quite different from those of the coefficients of the $\bar{\beta}^{-1}$ expansion: $C_1 \simeq 990$ and $C_3 \simeq 4.4$. With these values, the optimal order for $\beta = 6$ is 25.

The accuracy curves for the two models are compared in Figs. 14 and 15. We have used the known values for the first 10 coefficients. A careful examination shows that the

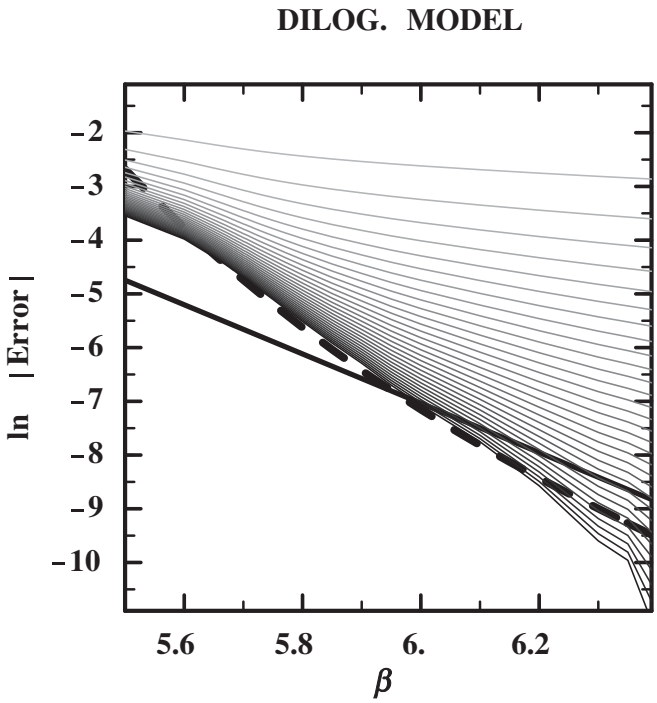

FIG. 14. Natural logarithm of the absolute value of the difference between the series and the numerical value for order 1 to 30 for quenched QCD with the dilogarithm model. As the order increases, the curves get darker. The long dashed curve is $\ln(0.65(a/r_0)^4)$. The solid curve is $\ln(3.1 \times 10^8 \times (\beta)^{204/121-1/2}e^{-(16\pi^2/33)\beta})$.

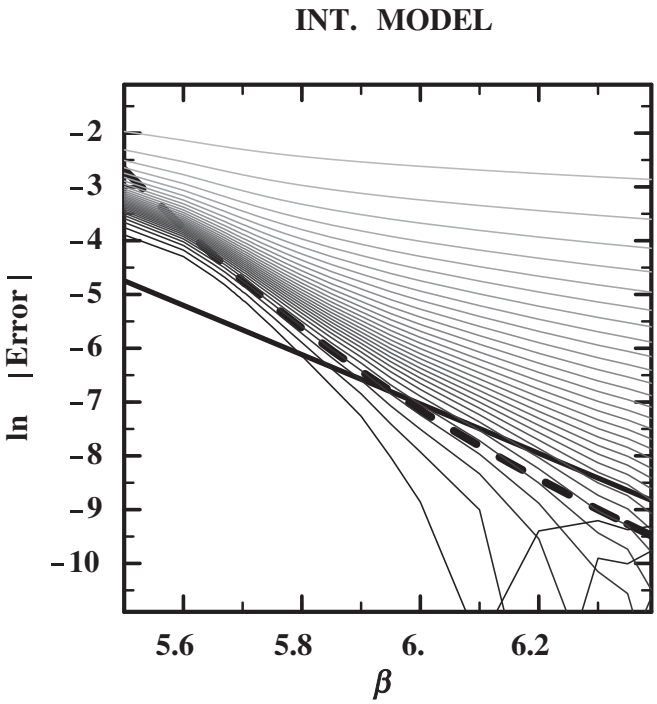

FIG. 15. Natural logarithm of the absolute value of the difference between the series and the numerical value for order 1 to 30 for quenched QCD with the integral model. As the order increases, the curves get darker. The long dashed curve is $\ln(0.65(a/r_0)^4)$. The solid curve is $\ln(3.1 \times 10^8 \times (\beta)^{204/121-1/2}e^{-(16\pi^2/33)\beta})$.

figures hardly differ up to order 25. From these two figures, it is plausible that the envelope of the true series is close to $0.65(a/r_0)^4$. This value of 0.65 does not correspond to a best fit procedure. If we had forced the $(a/r_0)^4$ behavior and fitted the proportionality constant at order 26, we would have obtained 0.79 for the dilogarithm model and 0.71 for the integral model. If we had plotted the corresponding curves in Figs. 14 and 15, they would hardly be visible on these black and white figures. By taking a slightly smaller value 0.65, we made the dash curve more easy to see. We could also have plotted the curve corresponding $0.4(a/r_0)^4$ that can be inferred from the graphs and the estimate of the gluon condensate of Ref. [7]. Such a curve would be -0.49 below the one we drew.

The tadpole improvement [24] could be another method to study the asymptotic envelope of the accuracy curves. One defines the new series

$$P \simeq \sum_{m=0}^{K} b_m \beta^{-m} = \sum_{m=0}^{K} e_m \beta_R^{-m} + O(\beta_R^{-K-1}) \tag{50}$$

with a new expansion parameter

$$\beta_R^{-1} = \beta^{-1} \frac{1}{1 - \sum_{m=0} b_m \beta^{-m}}. \tag{51}$$

The consistent sets of numerical values [3,7,25], show that the beginning of the series converges much faster. This is clear up to order 8. However, for larger orders, the dependence on the higher order coefficients of the original series due to powers of $1/(1 - \sum_{m=0} b_m \beta^{-m})$ at low orders in β_R makes the tadpole improved series almost as slow as the original series. In extracting the coefficient [7] of a^4, Rakow used a more sophisticated method where $1/(1 - \sum_{m=0} b_m \beta^{-m})$ is replaced by the improved series with a value of β_R determined numerically [26]. This procedure gives better perturbative estimates which explains that the constant of proportionality 0.4 is smaller than 0.65 as discussed above.

Instead of assuming the $(a/r_0)^4$ behavior, it is also possible to extract the power from linear fits of $\ln(|\Delta_k|)$ versus $\ln(a/r_0)$. For $k \leq 26$ the two extrapolations give similar fits near $\beta = 6$. For instance, Δ_{26} is $0.56(a/r_0)^{3.72}$ in the dilogarithm model and $0.63(a/r_0)^{3.90}$ for the integral model. For larger k, the constant of proportionality and the exponent keep increasing slowly for the dilogarithm model and the procedure becomes meaningless for the integral model. We now discuss in more detail the stability of this fitting procedure.

VIII. UNCERTAINTIES ON EXTRAPOLATIONS

We now discuss the effects of the uncertainties of the known coefficients on the extrapolations introduced in the previous section. The determination of the unknown parameters in both models depends only on a_9 and a_{10}. The errors on these coefficients are due to the finite volume and the numerical implementation of the stochastic perturbation theory. According to Ref. [2], from which we took the values of a_9 and a_{10} for a 24^4 lattice, the statistical errors on a_9 and a_{10} are close to 1% while the errors due to the finite volume are less than half a percent for the calculations on a 24^4 lattice.

We have studied the effects of small changes of the following form:

$$a_i \rightarrow a_i(1 + \delta_i), \tag{52}$$

for $i = 9$ and 10 on the determination of the parameters $\mathcal{A}$ (amplitude) and $\mathcal{S}$ (slope in a log-log plot) appearing in the approximate parametrization

$$\Delta_{26} \simeq \mathcal{A}(a/r_0)^{\mathcal{S}}, \tag{53}$$

which was our best estimate of the NPP of the plaquette in the previous section. With the sign convention for Δ_k in Eq. (3), i.e., the numerical value *minus* the series at order k, $\Delta_k > 0$ for $k \leq 10$. If the coefficients of the series are all positive and end up growing factorially, it is clear that, for a given β, there is some order for which the truncated series becomes larger than the numerical value and Δ_k becomes negative. This explains the downward spikes that are clearly visible for orders 29 and 30 of the integral model on Fig. 15. On the other hand, for the dilogarithm model, Δ_k remains positive as k increases, over the whole β interval for which Δ_k is larger than the errors on the numerical values of P.

When the value of the series becomes close to the numerical value, the errors on the Monte Carlo estimates of P become important. The numerical values that we have used for the fits of $\mathcal{A}$ and $\mathcal{S}$ have estimated errors [19] smaller than 5×10^{-5}. Consequently, the details of Figs. 14 and 15 below -10 on the y axis are meaningless.

We have performed fits of $\mathcal{A}$ and $\mathcal{S}$ using $\ln(|\Delta_{26}|)$ versus $\ln(a/r_0)$ for 18 values of β between 5.68 and 6.10. The quality of the fit can be assessed from

$$\chi_f \equiv \left((1/18) \sum_{i=1}^{18} (D_i / \ln(|\Delta_{26}(\beta_i)|))^2 \right)^{1/2}, \tag{54}$$

with

$$D_i = \ln(|\Delta_{26}(\beta_i)|) - \ln(\mathcal{A}) - \mathcal{S} \ln(a(\beta_i)/r_0). \tag{55}$$

χ_f give an estimate of the typical relative errors obtained with the fit.

It is also useful to assess how well a particular choice of parameters reproduces the known values of the known coefficients of order 8 and less. For this purpose we have defined

TABLE II. Values of C, β_m, $\mathcal{A}$, $\mathcal{S}$, χ_f, and χ_a defined in the text for the dilogarithm model, corresponding to various choices of δ_9 and δ_{10}. All the fits refer to a comparison with the 26th order.

δ_9	δ_{10}	C	β_m	$\mathcal{A}$	$\mathcal{S}$	χ_f	χ_a
0	0	0.0654	5.79	0.56	3.72	0.004	0.006
0.01	0.01	0.0661	5.79	0.60	3.81	0.005	0.006
−0.01	−0.01	0.0647	5.79	0.52	3.65	0.003	0.015
0.01	−0.01	0.0791	5.67	0.40	3.31	0.002	0.048
−0.01	0.01	0.0541	5.90	1.46	4.72	0.017	0.056
−0.005	0.005	0.0595	5.85	0.77	4.07	0.007	0.031

$$\chi_a \equiv \left((1/4)\sum_{j=5}^{8}[(a_j - a_j[a_9, a_{10}])/a_j]^2\right)^{1/2}, \qquad (56)$$

with $a_j[a_9, a_{10}]$ understood as the value of a_j obtained from the models after the unknown coefficients have been fixed using a_9 and a_{10}. We started at order 5 because the differences on lower orders are quite large for the integral model.

It is interesting to notice that, in both models, the extrapolated coefficients depend linearly on a overall scale factor called C in the dilogarithm model and C_1 in the integral model. These scale factors cancel if we consider the ratio of the two equations determining the unknown parameters. In other words, the parameters β_m and d_1 depend only on a_9/a_{10}. Consequently, if $\delta_9 = \delta_{10} = \delta$, a_9/a_{10} is unchanged and the only effect of the change is to rescale all the extrapolated coefficients by a common factor $1 + \delta$. This type of modification generates a linear response which is the same at all orders and has quite controllable effects. On the other hand, if $\delta_9 \neq \delta_{10}$, the parameters β_m and d_1 are modified and this has more drastic effects on the extrapolated coefficients.

In order to give a quantitative idea, we have considered the four cases corresponding to the condition $|\delta_9| = |\delta_{10}| = 0.01$. The results are shown in Tables II and III. The choice $\delta_9 = -0.01$ and $\delta_{10} = 0.01$ has a χ_f significantly larger than the other choices. For this choice, the two models start differing significantly at order lower than 26 and then develop negative spikes at larger order. It might have been a better choice to quote fits at lower order where there is a better agreement between the two models and smaller χ_f. For instance, at $k = 22$, we obtain $\mathcal{A} = 0.69$ and $\mathcal{S} = 3.90$ with $\chi_a = 0.007$ for the dilogarithm model and $\mathcal{A} = 0.61$ and $\mathcal{S} = 3.77$ with $\chi_a = 0.005$ for the integral model. As the fit for $k = 26$ did not look reasonable for this choice of δ_i, we also added a line with the same signs but a lower magnitude.

TABLE III. Values of C_1, $-d_1$, $\mathcal{A}$, $\mathcal{S}$, χ_f, and χ_a defined in the text for the integral model, corresponding to various choices of δ_9 and δ_{10}. All the fits refer to a comparison with the 26th order.

δ_9	δ_{10}	C_1	$-d_1$	$\mathcal{A}$	$\mathcal{S}$	χ_f	χ_a
0	0	0.219	3.82	0.63	3.90	0.004	0.08
0.01	0.01	0.221	3.82	0.70	4.01	0.006	0.07
−0.01	−0.01	0.216	3.82	0.57	3.81	0.003	0.08
0.01	−0.01	0.263	3.72	0.42	3.44	0.002	0.03
−0.01	0.01	0.182	3.92	2.29	5.24	0.024	0.12
−0.005	0.005	0.199	3.87	0.94	4.33	0.009	0.10

In summary, we obtained values of $\mathcal{S}$ between 3.3 and 4.3 for fits with a reasonable χ_f. The boundary of this interval corresponds to fits that have a larger χ_a. These results seem to favor the idea that the NPP scales like a^4 over the idea that the NPP scales like a^2. However, no strong conclusions can be drawn because the extrapolation models are empirical. The only indication of their approximate validity is that they provide consistent results up to some reasonably large order. It should also be pointed out that there is no universal agreement [5,27] about what should be done about the Landau pole in Eq. (44). In order to draw strong conclusions, one would need either numerical values of the coefficients up to significantly larger order than available now or extrapolation models supported by a detailed analysis of graphs having significant contributions in *lattice* perturbation theory.

IX. PARAMETRIZATION OF THE FORCE SCALE

In the previous section, we considered the possibility of having the minimal error proportional to the fourth power of the two-loop renormalization group invariant scale. What is attractive about this possibility is that it has the generic form $A\lambda^B e^{-C/\lambda}$. However, the extrapolations suggest that it is not a very accurate parametrization of the envelope of the accuracy curves and that a $(a/r_0)^4$ parametrization seems more promising. In this section, we consider simple parametrizations of a.

First we study the derivative of $\ln(a)$ with respect to β with the first two universal terms subtracted. It should be noted that the derivative emphasizes the cubic terms in the expansion of $\ln(a)$ and the difference between the two expansions from Refs. [9,10] is more pronounced than without the derivative (see Fig. 16). We propose the following parametrization:

$$d\ln(a/r_0)/d\beta = -(4\pi^2/33) + (51/121)\beta^{-1} + A_1 e^{-A_2\beta}. \qquad (57)$$

This form was originally motivated by our idea of obtaining a NPP that could be calculable semiclassically and was found later in good agreement with an independent argument [11] (see below). We have also tried power parametrizations of the form $B_1\beta^{B_2}$ and found that it requires a large value of B_2 (close to 16) not very stable under small

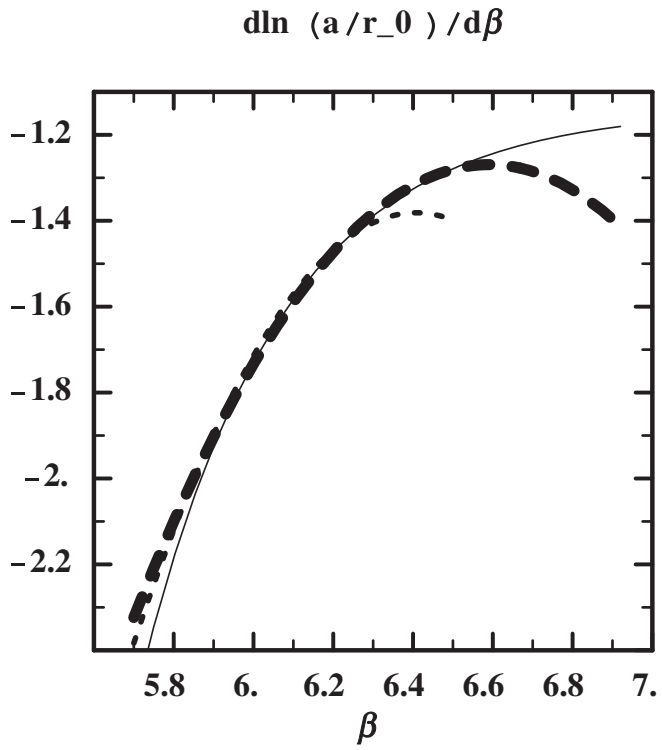

FIG. 16. $d\ln(a/r_0)/d\beta$ using Ref. [10] (thick dashes), [9] (small dashes), and Eq. (57) (solid line).

changes of the fitting interval. Using the Taylor expansion of Ref. [10] to produce a set of numerical values between 5.9 and 6.3, subtracting the first two terms of the right-hand side (rhs), and taking the log, we can determine numerically the parameters A_1 and A_2 from a linear fit. The result is $A_1 = -1.35 \times 10^7$ and $A_2 = 2.82$. For these values the exponential corrections become larger than the two universal terms for $\beta < 5.8$. Integrating and fitting the constant of integration in the same interval, we found

$$\ln(a/r_0) = A_3 - (4\pi^2/33)\beta + (51/121)\ln(\beta) - (A_1/A_2)\,\mathrm{e}^{-A_2\beta}, \tag{58}$$

with $A_3 = 4.5276$. This constant was obtained by plotting the left-hand side minus all the other terms of the rhs versus β. A nice plateau appears between $\beta = 5.9$ and 6.3. The extremal values in this interval are 4.5272 and 4.5282.

Note that the value of A_2 seems consistent with the idea [11] of using a^2_{pert} corrections for this quantity. The symbol a_{pert} refers to the one-loop or two-loop expression which in the short β interval considered here can hardly be distinguished from each other. For this reason, we have not introduced any power correction in the last term of Eq. (57). The assumption of a^2_{pert} corrections fixes $A_2 = 8\pi^2/33 \simeq 2.4$ which is close to the value 2.82 obtained above.

It is possible to use Eq. (58) to predict $\ln(a/r_0)$ at large β. For instance, at $\beta = 7.5$, we obtain -3.59 (for -3.63 in Ref. [28]) and -4.74 at $\beta = 8.5$ (for -4.81 in Ref. [28]). It is also possible to obtain the lattice scale Λ_L from the constant of integration A_3, namely $\Lambda_L = \exp(-A_3)/r_0 \simeq 4.4$ MeV.

X. CONCLUSIONS

We have considered the definition of the nonperturbative part of a quantity as the difference between its numerical value and the perturbative series truncated by dropping the order of minimal contribution (which is coupling dependent) and the higher orders. For the anharmonic oscillator, the double-well potential and the single plaquette gauge theory, the nonperturbative part can be parametrized as $A\lambda^B \mathrm{e}^{-C/\lambda}$ and the constants A, B, and C can be calculated analytically.

For lattice QCD in the quenched approximation, the perturbative series for the average plaquette is dominated at low order by a complex singularity and, at this point, the asymptotic behavior can only be reached by using extrapolations. We have considered two extrapolations that provide a consistent description of the series up to order 20–25. More work is needed to understand these extrapolations better. A diagrammatic interpretation of the dilogarithm formula should be possible. The similarities between the one plaquette integral and the renormalon motivated integral suggest that it might be possible to derive the latter from an effective action for a single plaquette, obtained from the large volume partition function after integrating over all the other links. Ultimately, the two approximations should be put together using dispersion relations in the complex β plane.

The two extrapolations favor the idea that the nonperturbative part is a power of the lattice spacing calculated using the force method and that the power is close to 4. We found a parametrization of the force scale as the two-loop universal terms with exponential corrections consistent with a^2_{pert} corrections. These corrections become quite important when β is near or below 6.

For large β, we can treat the exponential corrections as small quantities and expand in powers of these small quantities. The NPP of the plaquette is then written as a superposition of terms of the form $A_j\beta^{B_j}\mathrm{e}^{-C_j\beta}$. If the constants B_j and C_j can be determined from general arguments, we only need to determine the amplitudes A_j, starting from those with smallest C_j. Calculating more terms of the perturbative series and calculating more accurate numerical values of the average plaquette at large β would help in the empirical determination of these constants. As β becomes large, the lattice spacing becomes small and the NPP is small. It is plausible that the amplitudes could be calculated by semiclassical methods in the continuum. This is the most challenging part of the program. A method that comes to mind is the instanton

calculus. However, the infrared sensitivity of the procedure is notorious and phenomenological input such as the gluon condensate is often invoked to produce realistic formulas [29]. Having accurate empirical formulas for a well-defined model (quenched) lattice QCD would help to revisit this question from scratch.

ACKNOWLEDGMENTS

We acknowledge valuable discussions with C. Allton, M. Creutz, F. di Renzo, A. Duncan, G. Parisi, P. Rakow, and G. C. Rossi. This research was supported in part by the Department of Energy under Contract No. FG02-91ER40664.

[1] F. Dyson, Phys. Rev. **85**, 631 (1952).
[2] F. Di Renzo and L. Scorzato, J. High Energy Phys. 10 (2001) 038.
[3] L. Li and Y. Meurice, Phys. Rev. D **73**, 036006 (2006).
[4] A. H. Mueller, in Proceedings of the Workshop on QCD: 20 Years Later, Aachen, Germany, edited by P. M. Zerwas and H. A. Kastrup (World Scientific, Singapore, 1993).
[5] M. Shifman, *ITEP Lectures on Particle Physics and Field Theory* (World Scientific, River Edge, NJ, 2001).
[6] G. Burgio, F. Di Renzo, G. Marchesini, and E. Onofri, Phys. Lett. B **422**, 219 (1998).
[7] P. E. L. Rakow, Proc. Sci. LAT2005 (2006) 284 [hep-lat/0510046].
[8] R. Horsley, P. E. L. Rakow, and G. Schierholz, Nucl. Phys. B, Proc. Suppl. **106**, 870 (2002).
[9] M. Guagnelli, R. Sommer, and H. Wittig (ALPHA Collaboration), Nucl. Phys. **B535**, 389 (1998).
[10] S. Necco and R. Sommer, Nucl. Phys. **B622**, 328 (2002).
[11] C. R. Allton, hep-lat/9610016.
[12] A. Di Giacomo and G. C. Rossi, Phys. Lett. **100B**, 481 (1981).
[13] J. C. LeGuillou and J. Zinn-Justin, *Large-Order Behavior of Perturbation Theory* (North-Holland, Amsterdam, 1990).
[14] C. Bender and T. T. Wu, Phys. Rev. **184**, 1231 (1969).
[15] E. Brezin, J. L. Guillou, and J. Zinn-Justin, Phys. Rev. D **15**, 1544 (1977).
[16] S. Coleman, *Aspects of Symmetry* (Cambridge University Press, Cambridge, England, 1985).
[17] L. Li and Y. Meurice, Phys. Rev. D **71**, 054509 (2005).
[18] B. Alles, A. Feo, and H. Panagopoulos, Phys. Lett. B **426**, 361 (1998); **553**, 337(E) (2003).
[19] G. Boyd *et al.*, Nucl. Phys. **B469**, 419 (1996).
[20] H. D. Trottier, N. H. Shakespeare, G. P. Lepage, and P. B. Mackenzie, Phys. Rev. D **65**, 094502 (2002).
[21] G. Parisi, Lectures given at the 1977 Cargese Summer Institute, 1977.
[22] L. Li and Y. Meurice, Phys. Rev. D **71**, 016008 (2005).
[23] R. F. Dashen and D. J. Gross, Phys. Rev. D **23**, 2340 (1981).
[24] G. P. Lepage and P. B. Mackenzie, Phys. Rev. D **48**, 2250 (1993).
[25] L. Li and Y. Meurice, Proc. Sci. LAT2005 (2006) 258 [hep-lat/0509096].
[26] P. Rakow (private communication).
[27] G. Grunberg, hep-ph/9705290.
[28] M. Guagnelli, R. Petronzio, and N. Tantalo, Phys. Lett. B **548**, 58 (2002).
[29] T. Schafer and E. V. Shuryak, Rev. Mod. Phys. **70**, 323 (1998).